Pulsatile contractions and pattern formation in excitable active gels

Michael F. Staddon,[1] Edwin M. Munro,[2,3] and Shiladitya Banerjee[4,*]

[1]*Center for Systems Biology Dresden, 01307 Dresden, Germany*
[2]*Department of Molecular Genetics and Cell Biology, University of Chicago, Chicago, IL 60637, USA*
[3]*Institute for Biophysical Dynamics, University of Chicago, Chicago 60637, IL, USA*
[4]*Department of Physics, Carnegie Mellon University, Pittsburgh, PA 15213, USA*

The actin cortex is an active adaptive material, embedded with complex regulatory networks that can sense, generate and transmit mechanical forces. The cortex can exhibit a wide range of dynamic behaviours, from generating pulsatory contractions and traveling waves to forming highly organised structures such as ordered fibers, contractile rings and networks that must adapt to the local cellular environment. Despite the progress in characterising the biochemical and mechanical components of the actin cortex, our quantitative understanding of the emergent dynamics of this mechanochemical system is limited. Here we develop a mathematical model for the RhoA signalling network, the upstream regulator for actomyosin assembly and contractility, coupled to an active polymer gel, to investigate how the interplay between chemical signalling and mechanical forces govern the propagation of contractile stresses and patterns in the cortex. We demonstrate that mechanical feedback in the excitable RhoA system, through dilution and concentration of chemicals, acts to destabilise homogeneous states and robustly generate pulsatile contractions. While moderate active stresses generate spatial propagation of contraction pulses, higher active stresses assemble localised contractile structures. Moreover, mechanochemical feedback induces memory in the active gel, enabling long-range propagation of transient local signals.

Introduction.– The actin cortex is an adaptive active material that dynamically regulates its mechanical properties to maintain or change cell shapes [1–4]. Actin cortex can display a wide range of dynamic behaviours from driving intracellular pulsatory contractions [5, 6] to cellular-scale polarized flows [5, 7, 8] and assembling protrusive or contractile structures during cell motility and cytokinesis [9, 10]. These behaviours must adapt to the cell's local environment and developmental stage. For instance, cellular-scale pulsatile contractions are often observed during developmental morphogenesis, where pulsatile contractions act as a mechanical ratchet to sequentially alter cell size and shapes [11–14], leading to tissue bending or elongation [15]. At the intracellular level, these pulses can occur with chaotic spatiotemporal dynamics [5, 16, 17], or can have periodic spatiotemporal structures as seen in surface contraction waves in *Xenopus* embryos [18, 19]. In other physiological contexts, stable contractile structures are needed, as in the assembly of an actomyosin purse-string during wound healing [20], or the formation of a contractile ring during cytokinesis [21, 22]. While the biochemical pathways underlying actomyosin dynamics are known, the ways in which actomyosin-driven forces feedback to upstream chemical signals to govern cytoskeletal behaviours remain poorly understood [4].

Alan Turing, in his seminal paper, demonstrated that reaction-diffusion systems can autonomously generate a wide variety of spatiotemporal patterns observed in nature, but noted that mechanical forces may also play an important role in pattern formation [23]. In recent years, purely biochemical models have been proposed for actomyosin pattern formation. RhoA and its downstream effectors of actin and myosin have been shown to form an activator-inhibitor system that exhibits excitable dynamics and oscillations [17, 24, 25]. Here autocatalytic production of the activator RhoA leads to local accumulation of the inhibitor F-actin, which in turn limits the spreading of activators. This triggers the next cycle of autocatalytic production of RhoA, resulting in traveling waves [24, 25]. Since F-actin diffusion is negligible compared to RhoA, this model cannot spontaneously generate Turing patterns. By tuning RhoA production rates locally, static patterns of RhoA can be generated. This raises the question if actomyosin patterns strictly rely on biochemical cues or can spontaneously and robustly emerge via interactions with an active mechanical medium.

Mechanochemical feedback in the cytoskeleton is another mechanism for generating spatiotemporal patterns [26–29]. Active gel models of the cytoskeleton have suggested that pulsatory patterns can emerge from contractile instabilities driven by a positive feedback between active stress and advective flows generated by a stress regulating chemicals such as actin and myosin [28, 30, 31]. These contractile instabilities cluster myosin into a few high concentration regions, but regulating myosin contraction with an independent RhoA oscillator can prevent the collapse of myosin and sustain oscillations [32]. However recent studies suggest a negative feedback loop between actomyosin and RhoA [17, 24, 25], raising the question of how the feedback between RhoA and actomyosin mechanics are regulated to generate flows and patterns.

Here we develop a mathematical model for an excitable signalling network comprising RhoA and actomyosin, embedded in an active mechanical medium, to study how the feedback between biochemical signalling and mechanical stresses regulate patterns and flows in the actin cytoskeleton. We specifically ask how pulsatory flows arise from the coupling between a fast diffusing activator (RhoA) and a slow diffusing inhibitor (actomyosin), how mechanochemical feedbacks stabilise contractile instabilities into localised patterns, and how active stresses propagate local contractile signals. We find that mechanical feedback acts to destabilise stationary states to robustly generate pulsed contractions.

At high contractile activity, stable patterns of actomyosin emerge. Furthermore, the system encodes memory of transient perturbations that allows local signals to be translated into propagating contraction waves or stable patterns.

Mechanical feedback generates robust pulsatile contractions. – To elucidate the role of mechanical feedback in the dynamic behaviours and instabilities in the actin cortex, we first study a coarse-grained three-element ODE model for the coupling between RhoA, actomyosin and mechanical strain in the actomyosin network. Our model draws from recent experiments on *Xenopus* oocytes [24] and *C. elegans* embryos [17] that suggest that actomyosin pulsation is regulated by the excitable dynamics of RhoA GTPase – the upstream regulator of actomyosin tension and turnover. Local autocatalytic activation of RhoA drives rapid initiation of pulses, followed by actomyosin recruitment. As actomyosin concentrations increase, F-actin dependent accumulation of the RhoA GTPase-activating proteins RGA-3/4 terminate the pulse through a delayed negative feedback [17]. This activator-inhibitor coupling between RhoA-GTP (concentration r) and actomyosin (concentration m) is described by the following dynamics:

$$\dot{r} = R_r(r,m) - r\frac{\dot{u}}{1+u}\,, \tag{1}$$

$$\dot{m} = R_m(r,m) - m\frac{\dot{u}}{1+u}, \tag{2}$$

where R_r and R_m define the rates for the assembly of RhoA and actomyosin, and $u(t)$ is the mechanical strain (Fig. 1a). Here the effect of F-actin and myosin are represented by a single species – actomyosin – that encompasses the inhibitory feedback supplied by F-actin as well as active force generation by myosin (see below). The second term on the right hand sides of the above equations arise from mass conservation – concentrations increase as the cell contracts and decreases as the cell relaxes, providing an additional mechanical feedback between RhoA and actomyosin. The chemical reaction rates are given by:

$$R_r(r,m) = S + a\frac{r^n}{A^n + r^n} - g\frac{mr}{G+r}, \tag{3}$$

where S is the applied stimulus (or basal rate of RhoA production) representing the activity of Rho-GEF, a is the rate of autocatalytic production of RhoA, n is a Hill coefficient, and g is a negative feedback parameter arising from F-actin-driven accumulation of RGA-3/4 that lowers the level of RhoA-GTP. The rate of actomyosin production is given by:

$$R_m(r,m) = S_m + k_a r^2 - k_d m, \tag{4}$$

where S_m is the basal rate of actomyosin production, k_a is the actomyosin assembly rate and k_d is the disassembly rate. The chemical reactions are coupled to mechanical deformations in the cytoskeleton, described as an active viscoelastic material with strain $u(t)$ and dynamics given by:

$$Eu + \eta\dot{u} = -\sigma_a\frac{m}{m_0+m}, \tag{5}$$

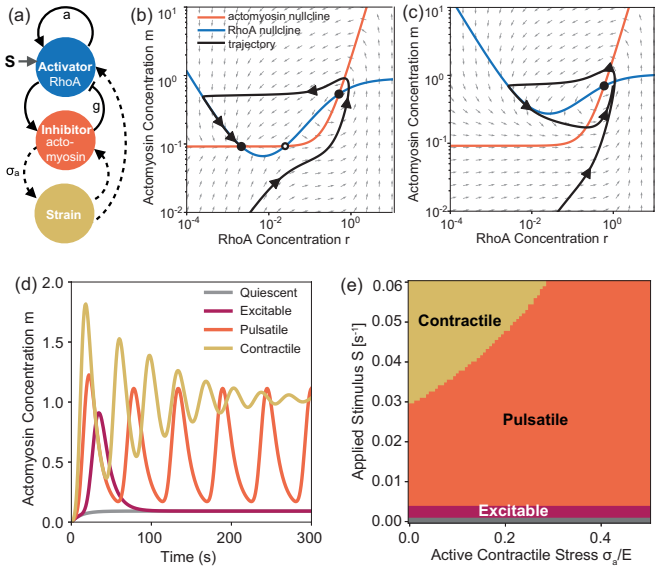

FIG. 1. Mechanical feedback sustains pulsatile contractions in excitable active medium. (a) Feedback loop schematic of the system. Solid lines indicate biochemical feedback. Dashed lines indicate mechanical feedback. (b-c) Trajectory curves and nullclines showing the fixed points for RhoA (blue) and actomyosin (orange) in the excitable (b) and in the pulsatile regime (c). Black arrows on the trajectory are equally spaced in time. Grey arrows show motion in phase space. Solid circles represent stable fixed points and the open circle is the unstable fixed point. (d) Concentration of actomyosin over time in the quiescent phase ($S = 0$), excitable phase ($S = 0.002$ s^{-1}), pulsatile phase ($S = 0.025$ s^{-1}), and contractile phase ($S = 0.075$ s^{-1}). (e) Phase diagram of the system, for varying contractile stress, σ_a/E, and applied stimulus, S, with $\eta/E = 5$s. See Table I in Supplemental Material for a list of default parameters in the model.

where E is the compressional elastic modulus, η is the viscosity, σ_a (> 0) is the maximum active stress arising from actomyosin-driven contractions, and m_0 is the concentration of actomyosin at half-maximum stress. While the mechanical parameters of the cortex are calibrated from available data [33], the model comes with several unknown reaction rate constants that we determine by fitting our model to the experimental time-series data of myosin and RhoA concentrations measured in the *C. elegans* cortex [17]. With these parameters calibrated, we simulate the system dynamics numerically [34], for different values of activity S and σ_a.

The model yields four distinct dynamic behaviours – quiescent, excitable, pulsatile, and contractile, depending on the magnitude of the applied stimulus, S (Fig. S1). For low S, the system displays an excitable behaviour – a single pulse of RhoA, followed by a pulse of actomyosin and contractile strain buildup, before reaching a steady-state (Fig. 1d). This excitable behaviour can be visualised in phase space as a trajectory about the intersecting nullclines (Fig. 1b). For this excitable pulse, we observed a loop about the high (r,m) fixed point before settling to a steady state at the lower fixed point.

As the applied stimulus is increased, other behaviours emerge (Fig. 1d-e). For a small increase in S, we observe sus-

tained pulsatile contractions, when the RhoA nullcline shifts up (Fig. 1c), resulting in a single fixed point at high concentrations and the system is trapped in a limit cycle. At even higher values of S, the limit cycle is unstable and the pulse amplitude decays until the system settles in a contracted state with high actomyosin concentration and strain. Finally, for very low applied stimulus, we observe a quiescent mode; both RhoA and actomyosin steadily increase to a fixed set-point.

While pulsatile contractions are observed in the absence of contractile stress ($\sigma_a = 0$), we find that including mechanical feedback helps to sustain oscillations over a wider range of the parameter space (Fig. 1e). As actomyosin drops after a pulse, the cell relaxes, further reducing both actomyosin and RhoA concentrations away from a fixed point, allowing another pulse to occur. Pulsatile contractions have been implicated in coordinating cell shape changes via a mechanical ratchet [35–37]. Mechanical feedback may be important in enabling robust control of this morphogenetic ratchet.

Spatial propagation of pulsatile flows and pattern formation.– To investigate the role of active mechanical stresses and RhoA signalling on the spatiotemporal regulation of actomyosin flows, we develop a continuum active gel model of the actin cortex, coupled to the excitable RhoA signalling network (Fig. 1a). The actin cortex is modelled as a one-dimensional Maxwell viscoelastic material, behaving elastically at short times and remodelling over longer time scales. Local balance of viscoelastic forces with cytosolic drag and actomyosin-generated active contractile forces can be written as:

$$\gamma(v + \tau\dot{v}) = \eta\partial_x^2 v + \sigma_a \partial_x \left(\frac{m}{m_0 + m}\right), \tag{6}$$

where $v(x,t)$ is the actin flow velocity, γ is the frictional drag coefficient, τ is the timescale for viscoelastic relaxation, η is the viscosity, σ_a is the active contractile stress, and m_0 is the actomyosin concentration at half-maximum stress.

Myosin-induced F-actin flows advect both RhoA and myosin, leading to their local accumulation due to convergent flows or depletion via divergent flows. These advective flows compete with reaction and diffusion of RhoA and actomyosin:

$$\dot{r} + \partial_x(rv) = R_r(r,m) + D_r\partial_x^2 r, \tag{7}$$

$$\dot{m} + \partial_x(mv) = R_m(r,m) + D_m\partial_x^2 m, \tag{8}$$

where D_r and D_m are the diffusion coefficients for RhoA and actomyosin, taken from Nishikawa et al [32]. The default parameter for active stress and viscoelastic time scale are taken from Saha et al [33]. The model equations are then numerically integrated [38] in a periodic box of length $L = 10\lambda$, where $\lambda = \sqrt{\eta/\gamma}$ is the hydrodynamic length scale. As shown in Fig. 2a-c, the numerical solutions predict a wide diversity of dynamic states as the active contractility $\sigma_a' = \sigma_a/\gamma$ and RhoA stimulus S are varied– from stationary patterns to propagating waves and pulsatile flows (Fig. S2).

At low σ_a', diffusion dominates over advection, giving rise to spatially uniform concentration profiles that exhibit excitable, oscillatory, or contractile dynamics (Fig. 2c, top row),

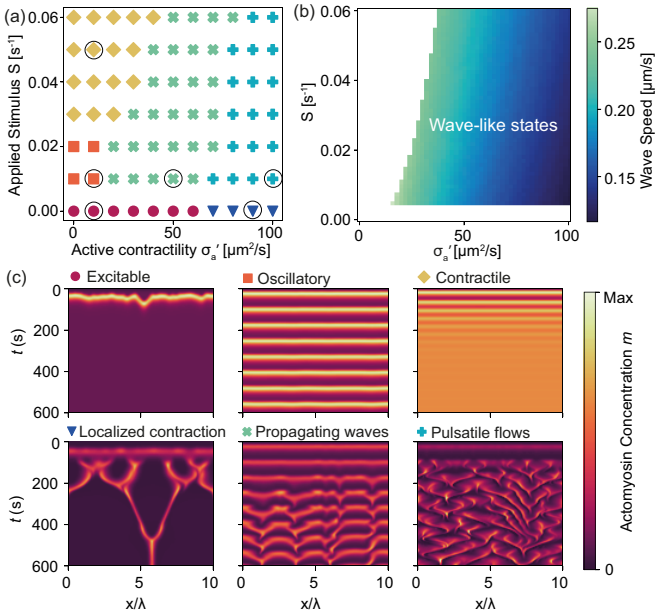

FIG. 2. Active stress generates spatial patterns and pulsatory flows. (a) Phase diagram of the dynamic states of the system as a function of applied Rho stimulus S and active contractility $\sigma_a' = \sigma_a/\gamma$. Encircled data points correspond to kymographs in panel (c). (b) Actomyosin wave speed, computed from linear stability analysis of the model equations, for varying S and σ_a'. (c) Kymograph of actomyosin concentration in different regimes (left to right, top to bottom): excitable, oscillatory, homogeneous contractile, localised contractions, propagating waves and pulsatile flows. See Supplemental Tables I and II for a list of model parameters.

as observed in the ODE model (Fig. 1). In the absence of mechanical feedback, reaction-diffusion alone cannot generate spatial patterns because the activator, RhoA, diffuses much faster than the inhibitor, actomyosin ($D_r \gg D_m$). When $D_r \ll D_m$, the homogeneous state becomes unstable and Turing patterns emerge (Fig. S3). This regime, however, is not realistic for the cortex since $D_r > D_m$. As σ_a' is increased, contractile instabilities develop due to local accumulation of actomyosin, allowing finite wavelength patterns to emerge.

At low S and high σ_a', we observe stable localized peaks of actomyosin and RhoA (Fig. 2c, bottom left). Initially, autocatalytic positive feedback of RhoA creates small RhoA concentration peaks (Fig. 3a, 1st panel), which in turn produce actomyosin (Fig. 3a, 2nd panel). As actomyosin begins to accumulate, large inward flows are generated, further increasing both RhoA and actomyosin concentrations (Fig. 3a, 3rd panel). Finally, actomyosin-induced inhibition of RhoA results in RhoA localization on either side of the actomyosin peak (Fig. 3a, 4th panel), in contrast to Turing patterns where activators and inhibitors overlap. With no RhoA advection, RhoA diffuses away from the peak, producing actomyosin behind it and generates a travelling wave (Fig. S4a). With no actomyosin advection, actomyosin concentrations remain too low to prevent RhoA from diffusing and create a uniform steady state (Fig. S4b). When several contractile actomyosin

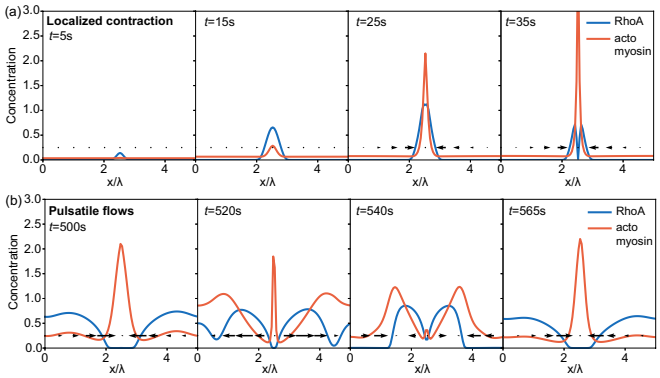

FIG. 3. Feedback mechanisms for pulsatile flows and stationary pattern formation. (a) RhoA and actomyosin concentration during localized contraction ($\sigma_a' = 80\ \mu\text{m}^2/\text{s}$, $S = 0$) at t = 5s, 15s, 25s, and 35s (left to right). (b) RhoA and actomyosin concentration profiles over a pulsatile flow cycle ($\sigma_a' = 80\ \mu\text{m}^2/\text{s}$, $S = 0.1\ \text{s}^{-1}$) at t = 500s, 520s, 540s, and 565s (left to right). Arrows indicate flow velocity.

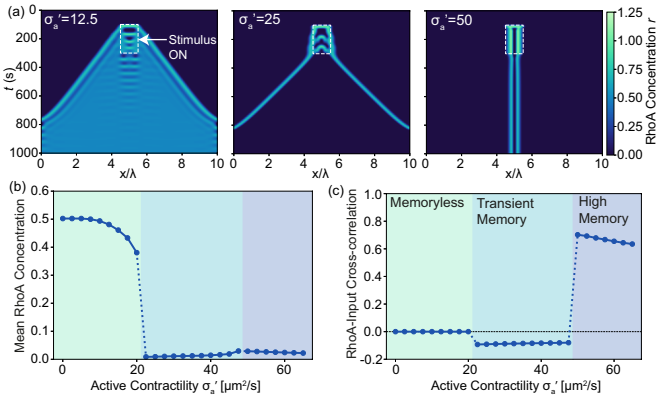

FIG. 4. Response to local bursts of contractile activity. (a) Kymograph of Rho concentration upon local transient application of Rho stimulus: $S = 0.03\ \text{s}^{-1}$ inside box (dashed rectangle) and $S = 0$ outside box, for different values of active stress: (left) bistable front propagation for $\sigma_a' = 12.5\ \mu\text{m}^2/\text{s}$, (middle) solitons for $\sigma_a' = 25\ \mu\text{m}^2/\text{s}$, and (right) localised contraction for $\sigma_a' = 50\ \mu\text{m}^2/\text{s}$. (b) Spatially averaged RhoA concentration, 300s after the application of stimulus. (c) Correlation between RhoA concentration and input stimulus $S(x,t)$, averaged over the last 120s.

foci exist, they attract each other and merge into a single peak.

At higher S and moderate σ_a', we observe propagating waves and pulsatile flows (Fig. 2c, bottom). A higher level of excitation in RhoA generates a localized actomyosin peak with high contractility. Away from the actomyosin peak, RhoA concentrations are higher and are advected towards actomyosin (Fig. 3b, 1st panel). Advected RhoA produces actomyosin as it moves, such that the newly assembled actomyosin generates flows away from the centre, reducing the actomyosin concentration at the centre (Fig. 3a, 2nd panel). Once the initial contraction dissipates, the two remaining actomyosin peaks merge, completing a cycle (Fig. 3a, panels 3-4). In propagating states, we observe periodic RhoA pulses, but as σ_a' is increased, actomyosin pulses generate large contractile flows that advect neighboring pulses, creating chaotic motion. Here, advection is necessary for the waves to form (Fig. S4d). Without advection of RhoA however, we may still observe waves, since the actomyosin generated by RhoA forms clusters that travel with RhoA (Fig. S4c). However, these waves display much less chaotic motion when compared to the system with advection (Fig. 2c, bottom right).

Linear stability analysis of the continuum model reveals the role of active stress in destabilising the homogeneous state of the system (Fig. 2b, Fig. S5). At low S, three fixed points exist (Fig. 1b), with the lower fixed point being stable for high σ_a'. As S is increased, the RhoA nullcline shifts up until only one fixed point remains and the system enters the pulsatile regime (Fig. 1c). Increasing σ_a' leads to contractile instabilities that manifest as propagating waves and pulsatile flows (Fig. 2c). While active stress is required for wave propagation, higher σ_a' leads to lower wave speeds (Fig. 2b).

Response to local bursts of contractile activity.– While our model can capture many of the dynamic states observed in the actin cortex, cells must have the ability to actively switch between flowing and contractile states during physiological transitions. Such state transitions may be triggered by a local up-regulation in RhoA activity, which may be induced in response to mechanical forces or by cell cycle checkpoints. It is unclear how local bursts in RhoA activity spatially propagates or for how long the effects of the signal persist.

To understand how RhoA signals can propagate through space and induce state transitions, we locally turned on RhoA activity and examined the output response. Starting from rest with no applied stimulus ($S = 0$), an increased stimulus is applied at the central region ($S = 0.03\ \text{s}^{-1}$) (Fig. 4a). By changing active stress in the system, we are able to regulate both the ability for the input RhoA to propagate in space, and for the system to remember the spatial location of the signal. We observed three distinct phases (Fig. 4a): (i) propagation of a bistable front, where the memory of the signal location is lost and a global increase in RhoA concentration is observed, (ii) a soliton phase with transient spatial memory, and (iii) a high memory phase where a stable RhoA pattern is maintained.

At low active stress ($\sigma_a' = 12.5\ \mu\text{m}^2/\text{s}$), RhoA is excited into a pulsatile state within the activation region, while spreading laterally through diffusion (Fig. 4a, left). A front of highly concentrated RhoA travels away from the source, increasing the total RhoA and actomyosin in the system (Fig. 4b). This is reminiscent of a bistable front propagation in classical excitable systems [39, 40], where the system switches to the high concentration stationary state (Fig. 2c).

As active stress is increased, we find that mechanical feedback is able to tune the properties of the biochemical system away from classical excitable systems. At moderate active stress ($\sigma_a' = 25\ \mu\text{m}^2/\text{s}$), RhoA pulses spread out as two solitons before annihilating as they meet (Fig. 4a, middle), as seen in surface contraction waves [18]. In contrast to classical excitable systems, actomyosin generated behind the RhoA

wavefront increases its own concentration through contractile flows. This region of highly concentrated actomyosin behind the wave acts as a barrier that inhibits RhoA, preventing the system from switching to the high fixed point, and instead creates a soliton. Such a barrier can be seen at σ_a', although it is too weak to prevent diffusion, with the band of reduced RhoA concentration behind the wavefront (Fig. 4a, left).

At high active stress ($\sigma_a' = 50\ \mu\text{m}^2/\text{s}$), the contractile forces within the activated region are strong enough to maintain a spatially localized state that persists after the activation, remaining stationary in a fixed location at the centre of activation (Fig. 4a, right). This suggests a potential mechanism for cells to direct the locations of contractility. Without the guidance of RhoA activation, the system in this parameter regime is incapable of spontaneously forming a stable pattern.

To quantify the input-output relationship of the system, we measured the correlation between the input signal and the output RhoA concentration at long times (Fig. 4c). At low σ_a', RhoA spreads outwards, leading to a loss of correlation between input and the output signal, akin to a memoryless system. For the soliton case, the shape of the input signal is remembered, resulting in a negative correlation as the waves travel away from the source. Finally, in the spatially patterned phase, a high-memory state emerges where RhoA remains localized at the centre of activation, with a strong positive correlation between the input and the output. These results suggest that mechanical stresses play an important role in biochemical signal propagation, and in retaining the spatial memory of activity. For low active stress, signals propagate the fastest with global changes in contractility and no memory of the spatial location of the signal. As active stress is increased, we observe contraction waves propagating away from the source, displaying transient memory. At higher stresses, a high memory state develops, where transient local RhoA activations create localized contractile states.

Discussion.– Chemical signalling and mechanical forces are both essential to regulate the dynamics of the cellular actin cortex. We demonstrate that mechanochemical couplings are necessary to generate waves, patterns and pulsatile dynamics in the actin cytoskeleton, with mechanical feedback helping to robustly sustain pulsatile contractions, and provide a new mechanism for spatial patterning of RhoA and actomyosin, distinct from classical Turing patterns [23]. At low RhoA activity and high contractile activity, actomyosin forms stationary patterns, with RhoA localized on either side of the actomyosin peak. At moderate RhoA activity and stress, we observe periodic waves of actomyosin which annihilate before new wavefronts are generated in regions with low actomyosin concentration (Fig. S2c). This is reminiscent of RhoA waves in starfish eggs [16]. As contractile activity is increased, the waves of actomyosin become highly peaked, generating pulsatile dynamics (Fig. S2c), reminiscent of pulsed contractions observed in the *C. elegans* cortex [5]. Besides generating patterns and flows, the level of active contractile stress regulates the system's response to local RhoA signals, enabling phase transitions and memory entrainment as the activity is increased. Together, these results show the importance of considering both mechanical forces and chemical reactions when modelling the actin cortex, and present several ways for cells to alter their dynamic mechanical behaviour.

* shiladtb@andrew.cmu.edu

[1] D. A. Fletcher and R. D. Mullins, Cell mechanics and the cytoskeleton, Nature **463**, 485 (2010).

[2] G. Salbreux, G. Charras, and E. Paluch, Actin cortex mechanics and cellular morphogenesis, Trends in cell biology **22**, 536 (2012).

[3] M. Murrell, P. W. Oakes, M. Lenz, and M. L. Gardel, Forcing cells into shape: the mechanics of actomyosin contractility, Nature Reviews Molecular Cell Biology **16**, 486 (2015).

[4] S. Banerjee, M. L. Gardel, and U. S. Schwarz, The actin cytoskeleton as an active adaptive material, Annual Review of Condensed Matter Physics **11**, 421 (2020).

[5] E. Munro, J. Nance, and J. R. Priess, Cortical flows powered by asymmetrical contraction transport par proteins to establish and maintain anterior-posterior polarity in the early c. elegans embryo, Developmental Cell **7**, 413 (2004).

[6] J. Sedzinski, M. Biro, A. Oswald, J.-Y. Tinevez, G. Salbreux, and E. Paluch, Polar actomyosin contractility destabilizes the position of the cytokinetic furrow, Nature **476**, 462 (2011).

[7] M. Rauzi, P.-F. Lenne, and T. Lecuit, Planar polarized actomyosin contractile flows control epithelial junction remodelling, Nature **468**, 1110 (2010).

[8] M. Mayer, M. Depken, J. S. Bois, F. Jülicher, and S. W. Grill, Anisotropies in cortical tension reveal the physical basis of polarizing cortical flows, Nature **467**, 617 (2010).

[9] L. Blanchoin, R. Boujemaa-Paterski, C. Sykes, and J. Plastino, Actin dynamics, architecture, and mechanics in cell motility, Physiological Reviews **94**, 235 (2014).

[10] T. Vignaud, C. Copos, C. Leterrier, Q. Tseng, L. Blanchoin, A. Mogilner, M. Théry, and L. Kurzawa, Stress fibers are embedded in a contractile cortical network, Nature Materials , 1 (2020).

[11] A. C. Martin, Pulsation and stabilization: contractile forces that underlie morphogenesis, Developmental biology **341**, 114 (2010).

[12] R. Fernandez-Gonzalez and J. A. Zallen, Oscillatory behaviors and hierarchical assembly of contractile structures in intercalating cells, Physical biology **8**, 045005 (2011).

[13] A. C. Martin, M. Kaschube, and E. F. Wieschaus, Pulsed contractions of an actin–myosin network drive apical constriction, Nature **457**, 495 (2009).

[14] G. B. Blanchard, J. Étienne, and N. Gorfinkiel, From pulsatile apicomedial contractility to effective epithelial mechanics, Current opinion in genetics & development **51**, 78 (2018).

[15] C. Bertet, L. Sulak, and T. Lecuit, Myosin-dependent junction remodelling controls planar cell intercalation and axis elongation, Nature **429**, 667 (2004).

[16] T. H. Tan, J. Liu, P. W. Miller, M. Tekant, J. Dunkel, and N. Fakhri, Topological turbulence in the membrane of a living cell, Nature Physics , 1 (2020).

[17] J. B. Michaux, F. B. Robin, W. M. McFadden, and E. M. Munro, Excitable rhoa dynamics drive pulsed contractions in the early c. elegans embryo, Journal of Cell Biology **217**, 4230 (2018).

[18] M. Yoneda, Y. Kobayakawa, H. Y. Kubota, and M. Sakai, Surface contraction waves in amphibian eggs, Journal of cell sci-

ence **54**, 35 (1982).

[19] J. Bischof, C. A. Brand, K. Somogyi, I. Májer, S. Thome, M. Mori, U. S. Schwarz, and P. Lénárt, A cdk1 gradient guides surface contraction waves in oocytes, Nature communications **8**, 1 (2017).

[20] W. M. Bement, C. A. Mandato, and M. N. Kirsch, Wound-induced assembly and closure of an actomyosin purse string in xenopus oocytes, Current biology **9**, 579 (1999).

[21] K. Murthy and P. Wadsworth, Myosin-ii-dependent localization and dynamics of f-actin during cytokinesis, Current biology **15**, 724 (2005).

[22] D. Vavylonis, J.-Q. Wu, S. Hao, B. O'Shaughnessy, and T. D. Pollard, Assembly mechanism of the contractile ring for cytokinesis by fission yeast, Science **319**, 97 (2008).

[23] A. Turing, The chemical basis of morphogenesis, Philosophical Transactions of the Royal Society of London. Series B, Biological Sciences **237**, 37 (1952).

[24] W. M. Bement, M. Leda, A. M. Moe, A. M. Kita, M. E. Larson, A. E. Golding, C. Pfeuti, K.-C. Su, A. L. Miller, A. B. Goryachev, *et al.*, Activator–inhibitor coupling between rho signalling and actin assembly makes the cell cortex an excitable medium, Nature cell biology **17**, 1471 (2015).

[25] A. B. Goryachev, M. Leda, A. L. Miller, G. von Dassow, and W. M. Bement, How to make a static cytokinetic furrow out of traveling excitable waves, Small GTPases **7**, 65 (2016).

[26] S. Banerjee and M. C. Marchetti, Instabilities and oscillations in isotropic active gels, Soft Matter **7**, 463 (2011).

[27] S. Banerjee, K. J. Utuje, and M. C. Marchetti, Propagating stress waves during epithelial expansion, Physical review letters **114**, 228101 (2015).

[28] J. S. Bois, F. Jülicher, and S. W. Grill, Pattern formation in active fluids, Physical review letters **106**, 028103 (2011).

[29] P. Gross, K. V. Kumar, and S. W. Grill, How active mechanics and regulatory biochemistry combine to form patterns in development, Annual Review of Biophysics **46**, 337 (2017).

[30] K. V. Kumar, J. S. Bois, F. Jülicher, and S. W. Grill, Pulsatory patterns in active fluids, Physical Review Letters **112**, 208101 (2014).

[31] D. S. Banerjee, A. Munjal, T. Lecuit, and M. Rao, Actomyosin pulsation and flows in an active elastomer with turnover and network remodeling, Nature communications **8**, 1 (2017).

[32] M. Nishikawa, S. R. Naganathan, F. Jülicher, and S. W. Grill, Controlling contractile instabilities in the actomyosin cortex, Elife **6**, e19595 (2017).

[33] A. Saha, M. Nishikawa, M. Behrndt, C.-P. Heisenberg, F. Jülicher, and S. W. Grill, Determining physical properties of the cell cortex, Biophysical journal **110**, 1421 (2016).

[34] P. Virtanen, R. Gommers, T. E. Oliphant, M. Haberland, T. Reddy, D. Cournapeau, E. Burovski, P. Peterson, W. Weckesser, J. Bright, *et al.*, Scipy 1.0: fundamental algorithms for scientific computing in python, Nature methods **17**, 261 (2020).

[35] A. C. Martin, Pulsation and stabilization: contractile forces that underlie morphogenesis, Developmental Biology **341**, 114 (2010).

[36] M. F. Staddon, K. E. Cavanaugh, E. M. Munro, M. L. Gardel, and S. Banerjee, Mechanosensitive junction remodeling promotes robust epithelial morphogenesis, Biophysical Journal **117**, 1739 (2019).

[37] K. E. Cavanaugh, M. F. Staddon, E. Munro, S. Banerjee, and M. L. Gardel, Rhoa mediates epithelial cell shape changes via mechanosensitive endocytosis, Developmental Cell **52**, 152 (2020).

[38] J. E. Guyer, D. Wheeler, and J. A. Warren, Fipy: Partial differential equations with python, Computing in Science & Engineering **11**, 6 (2009).

[39] R. Priya, G. A. Gomez, S. Budnar, S. Verma, H. L. Cox, N. A. Hamilton, and A. S. Yap, Feedback regulation through myosin ii confers robustness on rhoa signalling at e-cadherin junctions, Nature Cell Biology **17**, 1282 (2015).

[40] R. Priya, G. A. Gomez, S. Budnar, B. R. Acharya, A. Czirok, Z. Neufeld, *et al.*, Bistable front dynamics in a contractile medium: Travelling wave fronts and cortical advection define stable zones of rhoa signaling at epithelial adherens junctions, PLoS computational biology **13**, e1005411 (2017).